Proc. Natl. Acad. Sci. USA
Vol. 94, pp. 6741–6745, June 1997
Biophysics

Voltage gating of *Escherichia coli* porin channels: Role of the constriction loop

(β-barrel/outer membrane protein/site-directed mutagenesis/single-channel conductance/x-ray structure)

PRASHANT S. PHALE*, TILMAN SCHIRMER†, ALEXEJ PRILIPOV*, KUO-LONG LOU†, ARIANE HARDMEYER*, AND JURG P. ROSENBUSCH*‡

Departments of *Microbiology and †Structural Biology, Biozentrum, University of Basel, CH-4056 Basel, Switzerland

Communicated by George Feher, University of California at San Diego, La Jolla, CA, April 16, 1997 (received for review February 18, 1997)

ABSTRACT **In the homotrimeric OmpF porin from *Escherichia coli*, each channel is constricted by a loop protruding into the β-barrel of the monomer about halfway through the membrane. The water-filled channels exist in open or closed states, depending on the transmembrane potential. For the transition between these conformations, two fundamentally different mechanisms may be envisaged: a bulk movement of the constriction loop L3 or a redistribution of charges in the channel lumen. To distinguish between these hypotheses, nine mutant proteins were constructed on the basis of the high-resolution x-ray structure of the wild-type protein. Functional changes were monitored by measuring single-channel conductance and critical voltage of channel closing. Structural alterations were determined by x-ray analysis to resolutions between 3.1 and 2.1 Å. Tethering the tip of L3 to the barrel wall by a disulfide bridge (E117C/A333C), mobilizing L3 by perturbing its interaction with the barrel wall (D312N, S272A, E296L), or deleting residues at the tip of the loop (Δ116–120) did not alter appreciably the sensitivity of the channels to an external potential. A physical occlusion, due to a gross movement of L3, which would cause the channels to assume a closed conformation, can therefore be excluded.**

Outer membranes of *Escherichia coli* provide efficient protection from noxious agents in the environment, such as detergents, toxins, and proteolytic enzymes. Their asymmetrical structure, glycolipids in the outer leaflets and phospholipids in the inner, constitutes an impermeable barrier that requires diffusion pathways for the translocation of nutrients and metabolites. In Gram-negative bacteria, this task is accomplished largely by porins. In these trimeric proteins, with masses of 37,000 Da per subunit, each monomer consist of a β-barrel that harbors the water-filled transmembrane channel. The pathway is constricted by a loop (L3) which connects β-strands 5 and 6 of the barrel and protrudes into the channel lumen, narrowing it midway across the membrane to about 7 × 11 Å (Fig. 1). The passage of solutes across the channel is limited to small (<600 Da), polar molecules and is slightly cation-selective in OmpF porin (4). Only a few larger solutes require specialized translocation pathways (5). We have studied the structures of this protein to high resolution in both structural and functional terms (2, 3, 6–9).

The equilibrium between open and closed states of the channels depends on the applied voltage (7). This phenomenon is poorly understood (10), since the overall potential difference across the outer membrane has been found to be small (11). However, a significant electrostatic field exists parallel to the plane of the membrane in the constriction site (1, 6), and its constituent charges may be affected by an applied potential. This hypothesis is vindicated by the results obtained with replacements of ionizable groups by uncharged residues (2). Also, it has recently been described that polysaccharides (8), membrane-derived oligosaccharides (12), polycations (13), and variations of pH values (3) and pressure (14) may exert modulatory effects on the critical voltages (V_c), above which channels close, and which are characteristic for any particular porin (7, 9). These phenomena strongly argue in favor of a physiological significance of channel closing, which can be exploited as highly sensitive gauges for the properties of mutated porins. In mechanistic terms, channel closure may be conceived of as being due either to a concerted movement of loop L3 that would obstruct the pore physically or, alternatively, to a hindrance of ion flux by multiple subtle positional

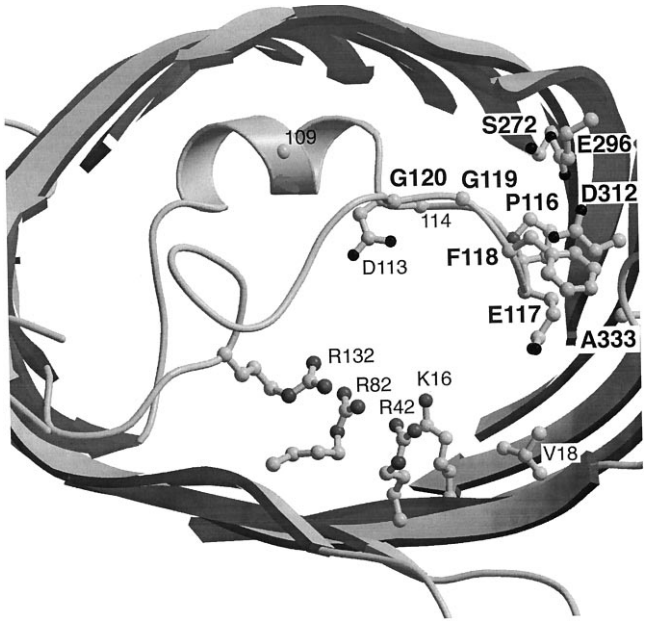

FIG. 1. Structure of the channel constriction in wild-type OmpF porin. The cationic cluster (Arg-42, Arg-82, Arg-132, Lys-16) and the two carboxyl side chains (Asp-113, Glu-117) on loop L3, which are the main source of the strong electrostatic field across the constriction (1), are shown. The amino acid sequence of loop L3 from residue 112 to residue 121 is TDMLPEFGGD. The loop is linked to the β-barrel wall by a chain of hydrogen bonds (Ser-272···Glu-296···Asp-312···backbone Glu-117/Phe-118). Other contact areas between wall and L3 consist of hydrophobic residues. Residues indicated in boldface are those mutated in the present study, while other positions (light labels) have been mutated and described previously (2, 3). The strands of the β-barrel (dark ribbons) are clipped to allow a full view of the channel constriction.

The publication costs of this article were defrayed in part by page charge payment. This article must therefore be hereby marked "*advertisement*" in accordance with 18 U.S.C. §1734 solely to indicate this fact.

‡To whom reprint requests should be addressed at: Biozentrum, University of Basel, Klingelbergstrasse 70, CH-4056 Basel, Switzerland. e-mail: rosenbusch@ubaclu.unibas.ch.

changes of fixed charges on the channel lining. As neither of the crystal structures determined so far could be identified as "closed" conformation (6, 15), molecular dynamics simulations (16) and analyses of the electrostatic field in the channel (1) have been performed. The models emerging favor either one or the other of these mechanisms.

We now have constructed nine site-specific mutant proteins on the basis of the wild-type porin structure to test these alternatives experimentally. In one case, the mutants presented were designed to allow formation of a disulfide bridge by which the constriction loop could be tethered to the barrel wall. In another case, (Δ116–120), the tip of L3 was deleted. Five more mutations were constructed to interfere with the interactions between constriction loop and barrel wall (Fig. 1, top right corner) by interrupting the chain of hydrogen bonds that exists in the wild-type protein and links the loop to the wall. The results presented here, which focus on the mechanism of closing, clearly demonstrate that none of the mutations drastically affects the sensitivity of the channels toward an applied potential.

MATERIALS AND METHODS

Bacterial Strains, Plasmids, Site-Directed Mutagenesis, Overexpression, and Porin Purification. *E. coli* strains used in this study were AK101 (17), DH5αmutS, and a BL21(DE3) derivative with *lamB*, *ompC*, and *ompA* genes deleted and the *ompF* gene inactivated by insertion of a Tn*5* transposon (A.P., unpublished work). Plasmids used were pTZ18urrh (17), pOmpF2, and pOmpF2urrh. The plasmid pOmpF2 is a pGEM-5zf(+) derivative containing the *ompF* gene under control of the T7 promoter. The orientation of the gene was the same as that of the amp^R gene. The plasmid pOmpF2urrh was derived by replacing the 5′ part of the β-lactamase gene (*bla*) and the origin of replication "ori" of the pOmpF2 plasmid by an analogous fragment from pTZ18urrh to introduce a 2-bp deletion into the "ori" region. The single-stranded DNA was purified from AK101 harboring pOmpF2urrh by using R408 helper phage (18). Site-directed mutagenesis was carried out as described (17, 19). The overexpression of mutant proteins was carried out in the *E. coli* BL21(DE3) derivative. Purification combined a procedure using negative extraction in SDS (20) with the purification (21, 22) in octyl-polyoxyethylene (octyl-POE; Alexis, Läufelfingen, Switzerland). The method yielded 2–3 mg of homogeneous OmpF porin per g of cells (wet weight).

X-Ray Structure Analysis and Functional Assays. Crystallization of mutant OmpF porins was carried out using the microdialysis method (22). The crystals (space group *P*321; typical size, 0.3 mm × 0.3 mm × 0.3 mm) were isomorphous to wild-type porin crystals, and the cell constants were set to wild-type values ($a = b = 118.5$ Å; $c = 52.7$ Å). The structures were determined by the difference Fourier technique based on the wild-type model (6). For the R_{free} calculations, the same test set as employed for the refinement of the wild-type structure was used. Refinement was performed with program REFMAC from the CCP4 suite (23), using the maximum likelihood function (MLKF) target.

Incorporation of wild-type protein into lipid bilayers yielded stable channels, with high cooperativity of initial steps (7, 24). Incorporation of mutant proteins E296Q/A/L, S272A, and A333C was very efficient, with little noise in the conductance traces. Incorporation of mutants D312N, E117C, E117C/A333C, and Δ116–120 was slightly less efficient, requiring application of potentials of 150–200 mV. Single-channel conductances (Λ) and critical voltages (V_c) were determined using positive and negative ramps. As the results with the two procedures did not differ significantly, only the values observed with positive ramps are shown (3, 25).

RESULTS

Electrical Properties of OmpF Mutants. Various mutants were constructed in OmpF porin (Tables 1 and 2). In comparison with wild-type porin, the reductions of the conductance values, observed with most of the point mutants, were moderate and rather uneventful. This also applied to the two cysteine mutants E117C and A333C, constructed either separately or in combination to yield E117C/A333C. Formation of a disulfide bridge was indicated by the changed mobility of the monomer band (not shown) in SDS/polyacrylamide gel electrophoresis and confirmed by structural analysis (see below). The values of single-channel conductance (Fig. 2) and threshold voltage in the cysteinyl double mutant under oxidizing conditions were intermediate to those of the two constituent single mutants. Preincubation with reducing agent caused a decrease of the conductance by 30%, but the V_c value was not affected by altering the state of oxidation of the protein. A deletion (Δ116–120), located at the tip of L3, showed a reduction of ion flux by 80%. In all mutants, the preference for cations over anions varied according to expectations, with a pattern comparable to that described previously (3). The results of the ion selectivities are, however, complex and are not immediately relevant in the present context. Their detailed analysis is therefore deferred (P.S.P., unpublished work). Here, the critical voltages of channel closing (V_c) provide the information that is crucial for distinguishing between the two closing mechanisms mentioned. The increase of the V_c values by 25–50% (Table 1) reveals that the channels of the mutant proteins are slightly more resistant to applied potentials than the wild-type protein, but that in no case are there drastic changes. This also includes the double mutant E117C/A333C.

Crystal Structures of Porin Mutants. The structures of seven of the mutants described above have been determined by x-ray analysis. Crystallographic details are given in Table 2. Mutants S272A, E296Q, and E296A show virtually no struc-

Table 1. Single-channel conductance and critical voltage of various OmpF mutants

Mutation	Λ, nS (*n*)	V_c, mV (*m*)
Wild-type		
OmpF	0.84 ± 0.06 (156)	145 ± 7 (10)
On barrel wall		
S272A	0.76 ± 0.02 (173)	196 ± 13 (15)
E296L	0.66 ± 0.04 (87)	202 ± 11 (17)
E296A	0.78 ± 0.03 (67)	172 ± 12 (14)
E296Q	0.78 ± 0.03 (63)	147 ± 10 (19)
D312N	0.60 ± 0.03 (137)	215 ± 15 (12)
A333C	0.81 ± 0.03 (50)	182 ± 17 (17)
On L3		
E117C	0.68 ± 0.02 (97)	199 ± 12 (15)
Δ116–120	0.17 ± 0.03 (90)	217 ± 14 (18)
L3 tethered to barrel wall		
E117C/A333C	0.71 ± 0.02 (159)	191 ± 12 (14)
Same, reduced	0.57 ± 0.01 (52)	198 ± 7 (8)

Values of the conductances (Λ), and those for the critical threshold voltages (V_c) are given with standard deviations. The number of events for the determinations of channel conductance is given in parentheses (*n*), and the number of experiments for the evaluation of V_c (over a voltage range of 0–230 mV) is also indicated in parentheses (*m*). For the determination of channel conductance, membranes with 5–7 trimers inserted were used. For the quantification of V_c, the number of trimers inserted into membranes was in the range of 15–20. For the double-Cys mutant, the channel properties were also determined by incubating the protein in 1 mM DTT for 10 min at room temperature prior to its incorporation into the planar bilayer. In these cases, DTT was present also in both compartments of the bilayer apparatus. Channel conductance was measured in 1 M NaCl/10 mM Tris·HCl/1 mM $CaCl_2$, final pH 7.4.

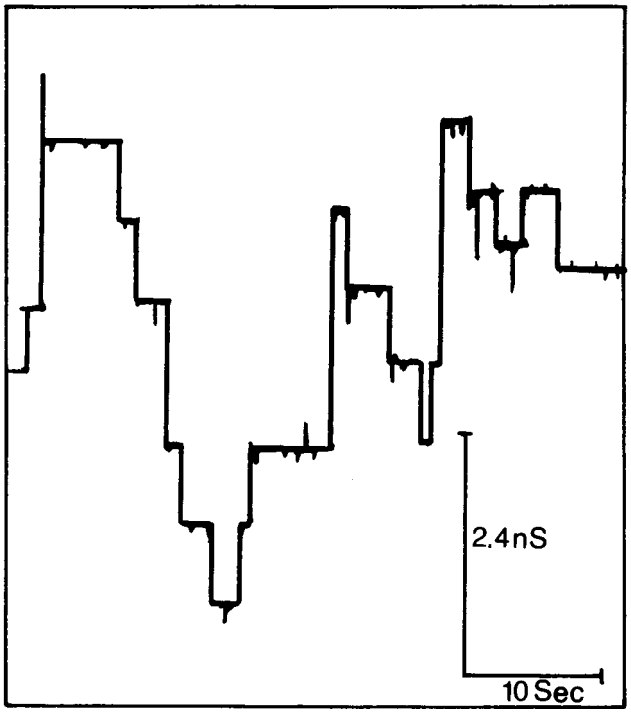

FIG. 2. Conductance trace of the S272A mutant of OmpF porin. Recording was obtained at +143 mV as described in *Materials and Methods* and previously (3). At the center of the trace, the cooperative activation of a trimer and its inactivation in three single steps is seen. The channel characteristics are qualitatively similar to those of wild-type OmpF porin, while quantitatively, small, yet distinct, differences exist (Table 1).

tural difference when compared with wild-type protein. In the last among them, a water molecule is observed in the space vacated by the truncated side chain (not shown). In mutant E296L (Fig. 3*A*), the distances to Ser-272 and Asp-312 are larger than in the wild type. This is due to a small concerted displacement of the side chain of Asp-312 which, together with the tip of L3, moves toward the channel lumen. The short hydrogen bonds between Asp-312 and main-chain amides 117 and 118 are conserved. In mutant D312N, the backbone at the tip of loop L3 (residues 115–119) adopts a new conformation and is detached by about 2.5 Å from the inner barrel wall (Fig. 3*B*). The electron density corresponding to the backbone of residues 117–120 does not show a unique conformation. There is no significant electron density corresponding to the side chains of Glu-117 and Phe-118. While the asparaginyl side chain of the mutated residue 312 is almost at the same position as the aspartyl side chain in wild type, the side chain of Glu-296 has changed its conformation considerably, but remains hydrogen bonded to residue 312 (Fig. 3*B*) and buried between L3 and the barrel wall. Asn-312 is now slightly exposed to solvent. The part of the β-barrel that is in contact with the tip of L3 in the wild-type structure has moved by 0.8 Å toward the channel lumen. To the best of our knowledge, this is the first among all OmpF mutants described so far for which a small but significant structural perturbation of the barrel scaffold has been observed.

The x-ray structure of the double-cysteine mutant E117C/A333C (Fig. 4) clearly shows that a disulfide bridge with the expected geometry has been formed. It is remarkable that no structural changes are observed elsewhere in the protein (see Table 2, last row). The structure of the deletion mutant Δ116–120 reveals a disrupted or absent electron density between residues 114 and 122. The rest of the structure is unchanged—i.e., the rms deviation of the positions of the atoms, when compared with the wild-type model, is within the limits of error.

DISCUSSION

Site-specific mutants in OmpF porin, in which the constriction loop L3 was either tethered to or loosened from the barrel wall, or was partially deleted, have been constructed. The effects of these alterations were determined by x-ray analysis and by single-channel recordings. The validity of the conductance studies (Table 1) compares well with that found in our previous bilayer experiments (3, 25), and the quality of the x-ray structure analysis is attested by the data shown in Table 2. The covalent attachment of the tip of L3 to the barrel wall by means of an engineered disulfide bridge was found to have a minor effect on the channel conductance, and it caused a 30% increase in the critical voltage V_c. Reduction of the disulfide bond did not affect V_c, but it did diminish the ion flux enough to warrant the conclusion that the disulfide bond was reduced. This was also supported by the differential mobilities of oxidized and reduced protein in polyacrylamide gel electrophoretic analysis in SDS (26). Significantly, the value of the threshold voltage in the oxidized form is not appreciably different from that observed for the two constituent single-cysteine mutants. Since the involvement of a major movement

Table 2. X-ray diffraction data of mutant OmpF porins

	Mutant						
Data	S272A	E296A	E296L	E296Q	D312N	Δ116–120	E117C/A333C
X-ray source	ESRF	ESRF	Basel	ESRF	Basel	Basel	Basel
Resolution, Å*	2.1	2.4	2.5	2.8	2.2	3.1	3.0
No. of unique reflections	24,276	16,831	14,272	10,688	21,639	7,631	8,527
R_{merge}, %	11.1	6.6	9.3	7.9	7.0	12.0	8.8
Completeness, %	91.4	98.4	96.6	97.6	97.6	95.8	96.8
Redundancy	1.8	3.3	5.5	2.9	7.6	3.0	2.5
R, %	21.0	17.7	18.7	18.5	20.3	22.4	18.6
R_{free}, %	27.1	25.7	26.2	26.8	25.4	32.4	27.1
rms deviation†							
Bond lengths, Å	0.018	0.017	0.014	0.009	0.019	0.012	0.008
Bond angles, °	0.043	0.044	0.041	0.034	0.043	0.044	0.031
rms deviation, mutant − wild type‡ Å	0.12	0.08	0.17	0.13	0.28	0.29	0.17

X-ray sources were a rotatory anode generator (Basel) or the Swiss–Norwegian beam line at the European Synchrotron Radiation Facility (ESRF) in Grenoble, France. All data were collected on Mar Research image plates.

*The low-resolution cutoff was 15 Å for all structures.

†rms deviation from ideal values.

‡rms deviation between all C^{α} positions of the mutant and wild-type model.

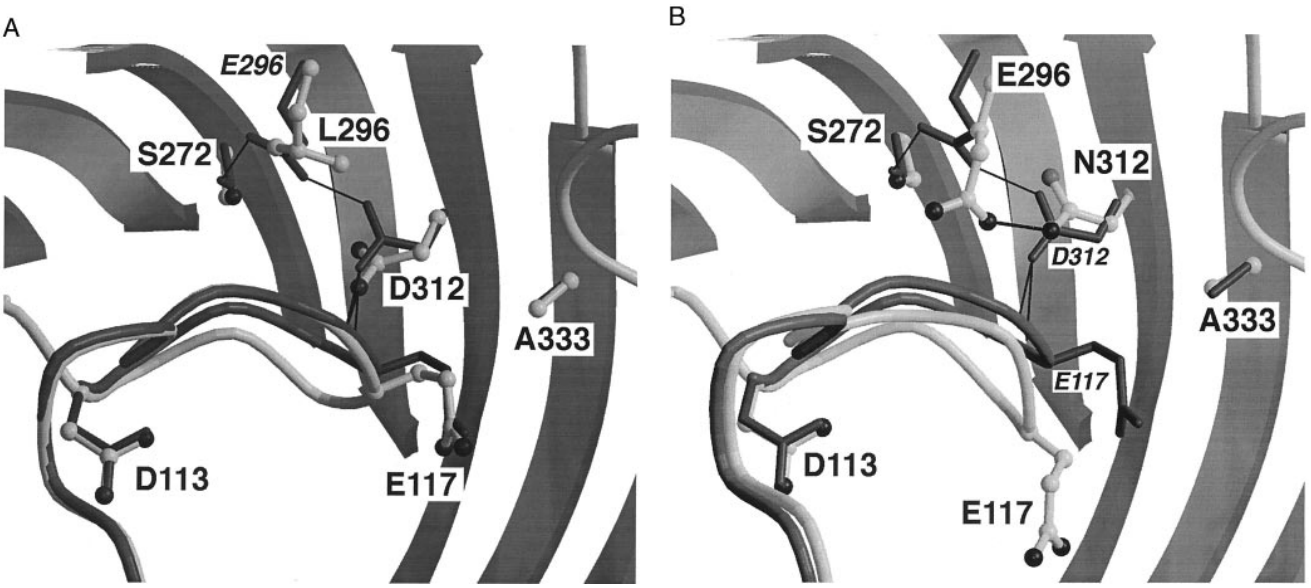

FIG. 3. Structure of the L3–barrel interface in OmpF porin mutants E296L (*A*) and D312N (*B*). For clarity, only the backbone of the constriction loop and the hydrogen bond network connecting L3 to the barrel are shown. Mutant structures are shown in gray ball-and-stick representation (residues labeled in boldface), with the superimposed wild-type porin structure shown as a black stick-model (residues labeled in italics). Potential hydrogen bonds are shown in thick (mutants) and thin (wild type) lines. The position of L3 is little affected by the E296L mutation (distance between the positions of wild-type and mutant $C^{\alpha}117 = 0.7$ Å), and the hydrogen bonds between Asp-312 and the backbone of L3 are conserved. In mutant D312N, L3 has moved toward the channel lumen by 2.5 Å and is partly detached from the barrel wall. Note that the side chain of Glu-117 is not defined by electron density.

of L3 in channel closing would be expected to cause a drastic decrease in voltage sensitivity, or an elimination of channel closure altogether, such a mechanism can be excluded.

As an independent and complementary test, loosening the interactions between L3 and the barrel wall by interfering with the hydrogen bond network (Fig. 1) would be expected to increase the responsiveness of the channels to applied potentials by allowing L3 to levitate more freely in the constriction zone. Structural changes, induced by the replacement of Glu-296 by the isosteric glutamine residue (E296Q), appear as uneventful as those in the E296L mutant, although in the latter, due to the lack of polar groups, hydrogen bonds could not form, and the distances to its neighbors are therefore enlarged. The negligible effects on the structure and function of the E296Q mutation corroborates an earlier calculation suggesting that Glu-296 is protonated in the wild-type protein, and hence uncharged (1). A rather drastic effect on the structure was observed for an analogous substitution, in which an aspartyl side chain is replaced by its amide derivative (D312N), as the tight interactions between the tip of L3 and the side chain are lost. Thus, in the wild-type protein, Asp-312 may be partially charged, and the abolishment of the charge in the mutant may weaken the hydrogen bonds with the backbone amides of Glu-117 and Phe-118 (at the tip of the loop). Due to the detachment of L3 from the barrel wall, an increase of channel sensitivity, and hence a decrease in the V_c value, might be expected, yet the reverse effect was observed. In the wild-type protein, the two buried acidic groups, Glu-296 and Asp-312, probably form "strong" or "low-barrier" hydrogen bonds (27) as have also been observed in other protein structures (28). In the third approach used, the tip of L3 was deleted (Δ116–120). X-ray analysis revealed disorder similar to

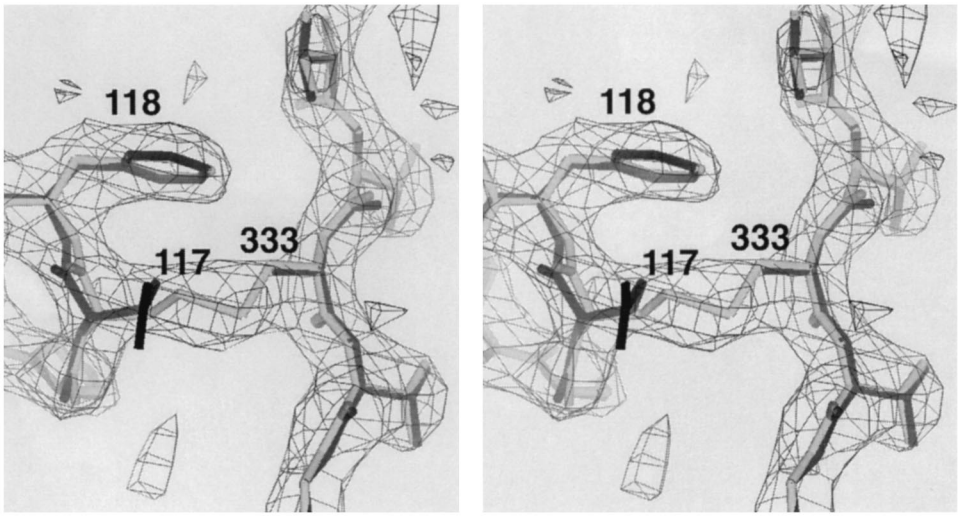

FIG. 4. Stereoscopic view of the engineered disulfide bond in OmpF mutant E117C/A333C. Superimposed on the $2F_o - F_c$ electron density map (contoured at 1σ) are the mutant (gray) and wild-type (black) models. Even in the close vicinity of the disulfide bridge, the mutant structure is virtually identical to wild type.

that described earlier for an adjacent deletion (Δ109–114; see ref. 2). Although the functional alterations are the most drastic among all the mutants reported here, the resulting disorder in the structure prevents detailed assignments. Thus, mutations which impair L3–barrel wall interactions are less sensitive to an external potential rather than more, a result that vindicates our conclusion, arrived at with the tethering experiment, that a gross movement of the constriction loop, as is predicted by molecular dynamics simulations (16, 29), can be ruled out as the mechanism for channel closure.

The results presented are, however, compatible with the alternative mechanism invoking multiple, subtle rearrangements of fixed charges in the lumen of the channel. In view of the observation that closed porin channels appear to allow water flux (30), and that an unrelated channel protein, aquaporin, facilitates water transport but is impermeant for ions (31), provides the incentive to study subtle changes in the distribution of fixed charges and the effects of shielding by mobile ions. Detailed predictions of such effects are in progress, using Poisson–Nernst–Planck simulations (32). Higher resolution should, moreover, provide information on the accessibility of water to pockets in the channel lining (e.g., between the barrel wall and L3), on changes in the state of the water structure in the channel constriction ["ice-like," "glass-like" (33)], as well as on altered hydrodynamic properties (34). Emerging models will, of course, be challenged by site-specific mutants.

We thank the staff of the Swiss–Norwegian beamline at the European Synchrotron Facility in Grenoble (France) for their assistance. The expert assistance of Gabriele Rummel and the critical reading of the manuscript by Dr. R. S. Eisenberg are most gratefully acknowledged. This work was supported by grants from the Swiss National Science Foundation to J.P.R. and T.S.

1. Karshikoff, A., Spassov, V., Cowan, S. A., Ladenstein, R. & Schirmer, T. (1994) *J. Mol. Biol.* **240,** 372–384.
2. Lou, K.-L., Saint, N., Prilipov, A., Rummel, G., Benson, S. A., Rosenbusch, J. P. & Schirmer, T. (1996) *J. Biol. Chem.* **271,** 20669–20675.
3. Saint, N., Lou, K.-L., Widmer, C., Luckey, M., Lou, K.-L., Schirmer, T. & Rosenbusch, J. P. (1996) *J. Biol. Chem.* **271,** 20676–20680.
4. Benz, R., Schmid, A. & Hancock, R. E. W. (1985) *J. Bacteriol.* **162,** 722–727.
5. Letellier, L. & Bonhivers, M. (1996) in *Transport Processes in Eukaryotic and Prokaryotic Organisms*, eds. Konings, W. N., Kaback, H. R. & Lolkema, J. S. (Elsevier, Amsterdam), Vol. 2, pp. 615–636.
6. Cowan, S. W., Schirmer, T., Rummel, G., Steiert, M., Ghosh, R., Pauptit, R. A., Jansonius, J. N. & Rosenbusch, J. P. (1992) *Nature (London)* **358,** 727–733.
7. Schindler, H. & Rosenbusch, J. P. (1978) *Proc. Natl. Acad. Sci. USA* **75,** 3751–3755.
8. Schindler, H. & Rosenbusch, J. P. (1981) *Proc. Natl. Acad. Sci. USA* **78,** 2302–2306.
9. Buehler, L. K., Kusumoto, S., Zhang, H. & Rosenbusch, J. P. (1991) *J. Biol. Chem.* **266,** 24446–24450.
10. Sen, K., Hellman, J. & Nikaido, H. (1988) *J. Biol. Chem.* **263,** 1182–1187.
11. Stock, J. B., Rauch, B. & Roseman, S. (1977) *J. Biol. Chem.* **252,** 7850–7861.
12. Delcour, A. H., Adler, J., Kung, C. & Martinac, B. (1992) *FEBS Lett.* **304,** 216–220.
13. Dela Vega, A. L. & Delcour, A. H. (1995) *EMBO J.* **14,** 6058–6065.
14. Le Dain, A. C., Häse, C. C., Tommassen, J. & Martinac, B. (1996) *EMBO J.* **15,** 3524–3528.
15. Cowan, S. W., Garavito, R. M., Jansonius, J. N., Jenkins, J., Karlsson, R., Koenig, N., Pai, E. F., Pauptit, R. A., Rizkallah, P. J., Rosenbusch, J. P., Rummel, G. & Schirmer, T. (1995) *Structure* **3,** 1041–1050.
16. Watanabe, M., Rosenbusch, J. P., Schirmer, T. & Karplus, M. (1997) *Biophys. J.* **72,** 2094–2102.
17. Ohmori, H. (1994) *Nucleic Acids Res.* **22,** 884–885.
18. Sambrook, J., Fritsch, E. F. & Maniatis, T. (1989) *Molecular Cloning: A Laboratory Manual* (Cold Spring Harbor Lab. Press, Plainview, NY), 2nd Ed.
19. Promega Corp. (1991) *Promega Protocols and Applications Guide* (Promega, Madison, WI), 2nd Ed.
20. Rosenbusch, J. P. (1974) *J. Biol. Chem.* **249,** 8019–8029.
21. Garavito, R. M. & Rosenbusch, J. P. (1986) *Methods Enzymol.* **125,** 309–328.
22. Pauptit, R. A., Zhang, H., Rummel, G., Schirmer, T., Jansonius, J. N. & Rosenbusch, J. P. (1991) *J. Mol. Biol.* **218,** 505–507.
23. Collaborative Computational Project Number 4 (1994) *Acta Cryst. D* **50,** 760–763.
24. Schindler, H. (1980) *FEBS Lett.* **122,** 77–79.
25. Saint, N., Prilipov, A., Hardmeyer, A., Lou, K.-L., Schirmer, T. & Rosenbusch, J. P. (1996) *Biochem. Biophys. Res. Commun.* **223,** 118–122.
26. Reynolds, J. A. & Tanford, C. (1970) *J. Biol. Chem.* **245,** 5161–5165.
27. Cleland, W. W. & Kreevoy, M. M. (1994) *Science* **264,** 1887–1890.
28. Flocco, M. M. & Mowbray, S. L. (1995) *J. Mol. Biol.* **254,** 96–105.
29. Björkstén, J., Soares, C. M., Nilsson, O. & Tapia, O. (1994) *Protein Eng.* **7,** 487–493.
30. Steiert, M. (1993) Ph.D. thesis (Univ. of Basel, Switzerland).
31. Jung, J. S., Preston, G. M., Smith, B. L., Guggino, W. B. & Agre, P. (1994) *J. Biol. Chem.* **269,** 14648–14654.
32. Eisenberg, R. S., Klosek, M. M. & Schuss, Z. (1995) *J. Chem. Phys.* **102,** 1767–1780.
33. Green, M. E. & Lewis, J. (1991) *Biophys. J.* **59,** 419–426.
34. Chen, D., Lear, J. & Eisenberg, R. S. (1997) *Biophys. J.* **72,** 97–116.